Orographic precipitation and kinematic flow structures of winter storms over the U.S. Pacific Northwest

Sandra E. Yuter[1*], M. Jordan Payne[1], David A. Stark[1], and Brian A. Colle[2]
[1]North Carolina State University, Raleigh, NC
[2]Stony Brook University, Stony Brook, NY

Introduction and Background

- Goals: 1. Test reproducibility of precipitation climatologies from other mountainous locations.

  2. Examine the sensitivity of locations of favored orographic enhancement over the U.S. Pacific Northwest to the stability, total storm volume, and the reflectivity threshold used to characterize the precipitation pattern.
- Portland was selected for its high frequency of orographic precipitation events, proximity of local operational radar and upper-air sounding sites, and its location relative to topography.

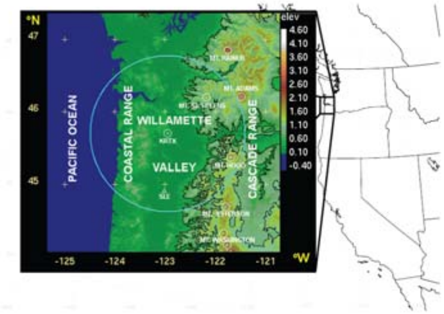

Figure 1: Topography of Portland, Oregon and its surrounding areas (km MSL altitude). Locations of the Coastal and Cascade Ranges, Portland WSR-88D with 120 km range ring, Salem sounding (triangle), and Willamette Valley are labeled.

Methodology

- This study follows the general methodology for identifying heavy rain events and analyzing characteristics of operational three-dimensional radar data used in James and Houze (2005).
- Storm days were selected based on daily rainfall totals of at least 5 mm from the Portland, OR airport. Surrounding days that accumulated at least 2.5 mm were also included with the storm event.
- Level II NEXRAD WSR-88D radar observations for the Portland, OR radar (KRTX) were obtained for the selected 117 storms from the National Climatic Data Center (NCDC)
- Radar reflectivity (dBZ), radial velocity (Vr), and precipitation frequency were calculated and analyzed for each storm.
- To mitigate contamination from the bright band, precipitation echo frequency with thresholds of Z ≥ 13 dBZ and Z ≥ 25 dBZ were used to describe the three-dimensional precipitation structures.
- The Salem, OR upper-air sounding (SLE) data were examined. Data were grouped by wind direction, stability (squared-moist Brunt-Väisälä frequency(N_m^2), and time-accumulated storm total precipitation echo volume.

Data Set

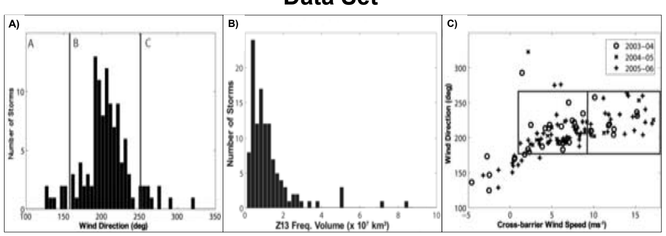

Figure 2: (A) Vertically-averaged wind direction between the 0.61-2.2 km altitude layer from SLE upper air soundings for 117 storms over three winter seasons. Black lines separate wind direction categories: A – SE storms (9), B – S-SW storms (98), and C – W-NW storms (10). (B) Histogram of storm total precipitation echo volume (Z >13 dBZ) over the three winter seasons. (C) Vertically averaged cross-barrier wind speed versus wind direction for layer. The box highlights storms for 180-260 azimuth layer averaged wind direction.

Data and Analysis

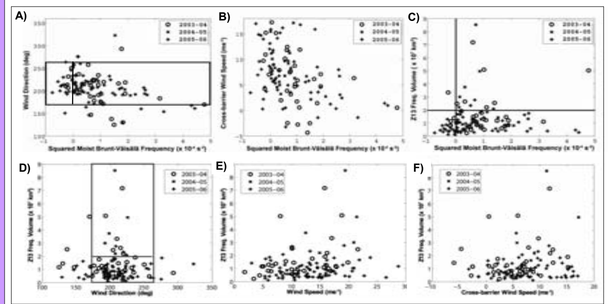

Figure 3: (A) Vertically averaged squared moist Brunt-Väisälä frequency vs vertically averaged wind direction, (B) vertically averaged cross-barrier wind speed, and (C) storm total precipitation echo volume (Z ≥ 13 dBZ). (D) Storm total precipitation echo volume (Z ≥ 13 dBZ) vs vertically averaged wind direction, (E) vs vertically averaged wind speed, and (F) vs cross-barrier wind speed. The box in (A) and (D) highlights the storms for 180° - 260° azimuth layer-averaged wind direction. The vertical line in (A) and (C) indicates separation of unstable ($N_m^2 < 0$) and stable/neutral ($N_m^2 \geq 0$). The horizontal line in (C) and (D) represents separation between large and small storms.

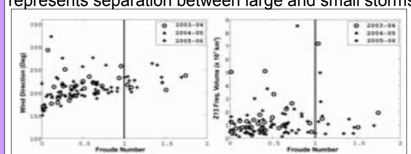

Figure 4: (A) Froude number vs vertically averaged wind direction and (B) storm total precipitation echo volume (Z ≥ 13 dBZ).

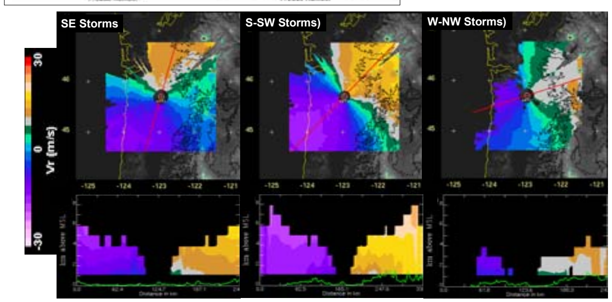

Figure 5: Comparison of radial velocity structures for storms with different low-level wind directions as defined in Figure 2a. Top plots are horizontal maps of mean radial velocity pattern at 2 km altitude. Bottom plots are vertical cross-sections of mean radial velocity along red lines in horizontal maps.

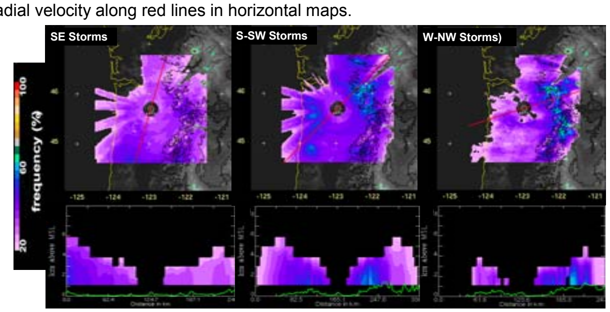

Figure 6: Three-dimensional precipitation echo frequency Z > 13 dBZ for storms with different low-level wind directions as defined in Figure 2a. Top plots are horizontal pattern at 2 km altitude. Bottom plots are vertical cross-section through red line in corresponding horizontal map.

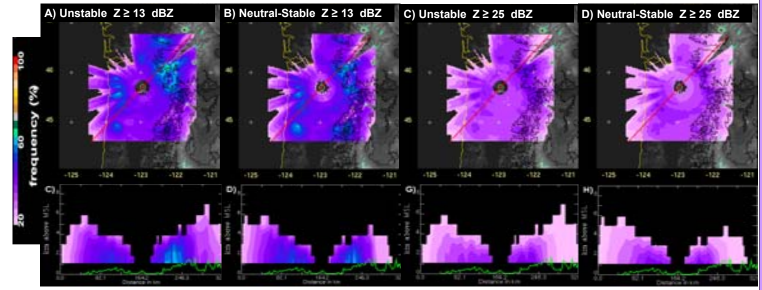

Figure 7: (A and C) Three-dimensional precipitation echo frequency for unstable storms and (B and D) neutral-stable storms with low-level winds from 180°-260° azimuth. (A and C) for precipitation frequency of Z ≥ 13 dBZ and (C and D) for precipitation frequency of Z ≥ 25 dBZ. The same threshold of 20% precipitation frequency at Z ≥ 13 dBZ is applied to both the Z ≥ 13 dBZ and Z ≥ 25 dBZ frequency plots.

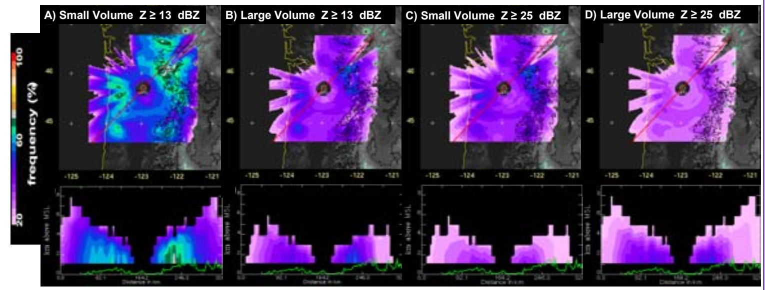

Figure 8: (A and C) Three-dimensional precipitation frequency for large volume and (B and D) small volume storms with low-level winds from 180°-260° azimuth. (A and B) for precipitation frequency of Z ≥ 13 dBZ and (C and D) for precipitation frequency of Z ≥ 25 dBZ.

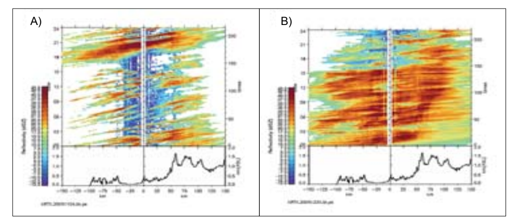

Figure 9: (A) Time versus distance plots of radar reflectivity at 2 km altitude along the E-W line at 45.35° N latitude for 2005 Nov 4 (small volume storm) and (B) 2005 Dec 30 (large volume storm).

Conclusions

- South and southwesterly storms represent 84% of storms in the Portland region.
- The distribution of storm volumes was strongly skewed toward smaller storms which had a wide range of stability, wind direction, and Froude number characteristics
- Larger volume storms (> 2 x 10^7 km^3) in the Portland region generally had winds from the southwest.
- Locations of favored precipitation enhancement along the windward slope of the Cascades occurred over different peaks depending on wind direction and stability.
- Depending on which minimum Z threshold (Z ≥ 13 or Z ≥ 25) was used, the number of local maxima in precipitation frequency and their locations differ relative to the underlying ridges and valleys.
- The complex, multi-ridge, three dimensional topography of the Cascades yields a superposition of localized enhancements.

Acknowledgements

This work was funded by National Science Foundation grants ATM-0549766 and ATM-0450444